



A Fracture-Mechanics Perspective on SBS–Glass Fiber Asphalt Concrete: Experimental SCB Results and Performance Indices

Sameer Abbas Jasim¹, Hasan Al-Mosawe²

^{1,2} Department of Civil Engineering, College of Engineering, Al-Nahrain University, Baghdad, Iraq.

ARTICLE INFO

Article history:

Received 26 December 2025
 Revised 26 December 2025,
 Accepted 18 January 2026,
 Available online 19 January 2026

Keywords:

Asphalt Fracture Toughness
 Modified reinforced asphalt
 Mixture Volumetric Properties
 Semi-circular Bending test
 Linear Elastic Fracture Mechanism

ABSTRACT

This study examined the influence of styrene–butadiene–styrene polymer and short glass fibers on the volumetric and fracture behavior of asphalt concrete prepared with locally sourced materials. Mixtures were designed using Marshall procedures to determine the optimum asphalt content and to verify conformity with Iraqi surface-course requirements. Polymer dosages of 2%, 4%, and 6% of binder mass were evaluated, and the optimum polymer level was subsequently combined with several glass-fiber contents. Fracture performance was assessed using semi-circular bending at 15 °C and interpreted through linear elastic fracture mechanics using maximum stress, maximum strain, fracture toughness, and stiffness index. In addition, a fracture toughness modulation index and an energy-based brittleness index were calculated from the load–displacement response to describe post-peak energy dissipation and relative brittleness. The results showed that polymer modification reduced the optimum asphalt content and increased Marshall stability; however, the 6% polymer mixture did not meet the flow requirement. Glass fibers improved Marshall stability up to an intermediate dosage and then reduced stability at higher contents. In the semi-circular bending test, glass fibers increased fracture toughness by about 30% relative to the conventional mixture, whereas polymer modification increased fracture toughness by about 125%. The hybrid polymer–fiber mixture achieved the highest fracture toughness (about 191% above the conventional mixture) and the highest stiffness index, indicating a combined benefit of improved ductility and crack-bridging reinforcement.

1. Introduction

Factors such as heavy traffic, sudden temperature fluctuations or very low temperatures can cause the rapid deterioration of the road pavement and significantly reduce its service life [1]. Scientists and engineers are constantly seeking new materials and technologies to enhance the durability and resilience of asphalt mixtures. The utilization of fibers in asphalt mixes has

been a common field of study in recent years due to their ability to improve mechanical performance and make other positive contributions [2], [3]. The potential for enhancing the mechanical properties of pavement and extending its lifespan significantly exists through the incorporation of fibers into asphalt mixtures, with outcomes varying based on the chosen fiber type and content [4], [5]. SBS is a triblock copolymer composed of styrene and butadiene as monomers and is the world largest thermoplastic elastomer with the most similar

Corresponding author : Samir.civ23@coeng.nahrainuniv.edu.iq
<https://doi.org/10.61268/54vtr333>

This work is an open-access article distributed under a CC BY license (Creative Commons Attribution 4.0 International) under

<https://creativecommons.org/licenses/by-nc-sa/4.0/> 

properties to rubber. SBS-modified asphalt is the most widely used type of modified asphalt in the world, and its research is also relatively extensive and in-depth. SBS can improve the rutting resistance of asphalt mixture [6], [7] and enhance low-temperature cracking resistance [8], [9], fatigue cracking resistance [10], [11], [12], and water damage resistance [13], [14]. Therefore, this kind of asphalt is also used in the highest proportion in highway engineering construction and occupies an absolute advantage in highway application.

Glass fiber is synthetic with high tensile strength, and its Young's modulus is nearly 70 GPa. Using glass fiber for modifying asphalt mixtures results in improved stability, durability, and ductility due to its high mechanical properties. Moreover, it increases the flow value and resistance to crack propagation in the mixture. At low temperatures, glass fiber can resist the cracks of the pavement as it has a potential resistance towards crack initiation [15], [16].

The SCB test has been utilised for evaluating the fracture performance of different modified asphalt mixtures at different test temperatures, loading modes, and loading rates. For instance, [17] used the SCB test to show the fracture effect and the role of modified asphalt to fracture toughness [17], [18], [19].

On other hand, some researches [20] used the SCB test to show the role of reclaimed asphalt and recycled materials on the fracture properties [21]. Huang used the SCB to evaluate the crack growth properties of asphalt mixtures under different test configurations, including test temperature and loading rate. The success in generating the requisite parameters for fracture assessment has ensued in developing the SCB

standard protocol for monotonic loading conditions [22], [23].

The purpose of this research is to evaluate and produce new of parameters semi-circular results based on load-displacement curve. And invent new evaluation method with high sensitivity to the modification of asphalt mixture.

2. Methodology

Two types of modification materials blended with conventional asphalt mixture. The blended amount founded by Marshall volumetric properties. The modified mixtures evaluated with Semi-circular bending test and new test parameters. The research methodology can be as shown in Figure 1.

3. Materials

Several materials were used in this research. Some of these materials are locally sourced, while others were imported for scientific research or industrial purposes. The materials are listed below.

3.1 Asphalt Cement

The material was prepared locally from the Al-Dorah refinery, Table 1 shows the physical properties of the asphalt.

3.2 Aggregates

The material was sourced locally from the Al-Naba'i site. The physical properties of the aggregates are shown in Table 2.

3.3 Mineral Filler

Limestone dust was used as a filler due to its chemical inertness. The material was prepared locally, and the physical properties of the limestone dust are listed in Table 3.

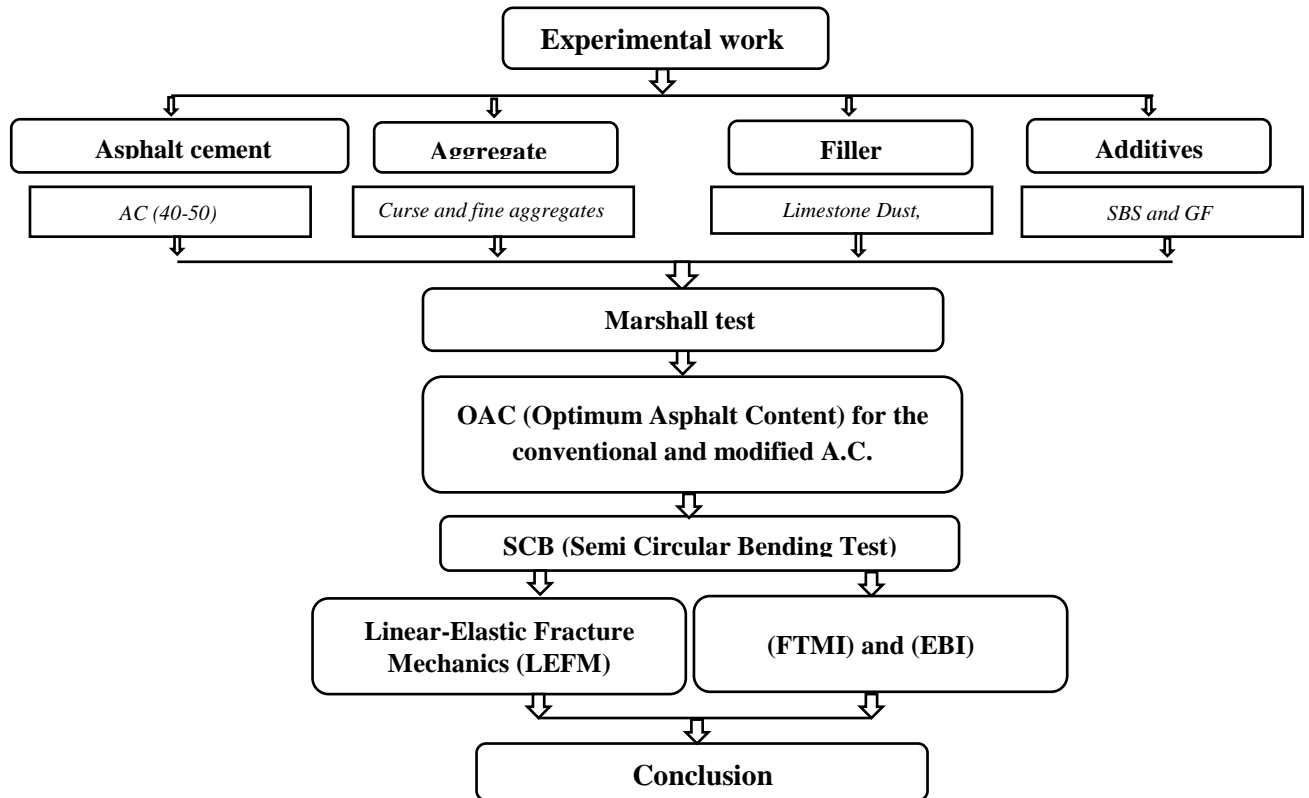


Figure 1. Work methodology flow chart.

3.4 Additives

3.4.1 SBS (Styrene-Butadiene-Styrene)

Styrene-butadiene-styrene (SBS) block copolymers are fascinating architecturally, where rigid polystyrene domains physically crosslink a rubbery polybutadiene matrix. This nanoscale morphology, a direct consequence of thermodynamic incompatibility, grants SBS its remarkable elasticity and strength, making it indispensable in applications ranging from high-performance footwear to sustainable asphalt modification. The material supplied from KRATON France company. The Physical and mechanical properties of the material listed in table 4. Figure 2 show the SBS material that used in this research.

3.4.2. Glass Fibers (GF)

Glass fiber is an inorganic short fiber. Glass fiber efficiently alters water stability and low-

temperature resilience. The product supplied by JUSHI Group company in China, and the product type (562A). The properties of glass fibers are shown in Table 5. Figure 3 shows the glass fibers used in this research.

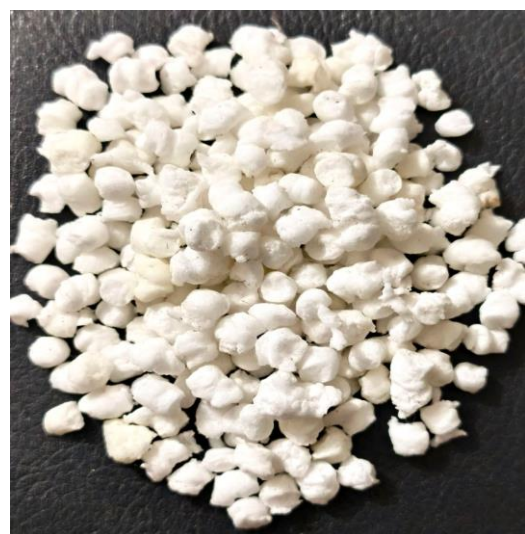


Figure 2. SBS used in this research.

Table 1: physical properties of the asphalt cement (40-50)

Test	units	Results	SCRB 2003 Specification Limits	ASTM Specification No.
Penetration (25 °C, 100 g, 5 sec)	1/10 mm	44	40 - 50	D5-06
Ductility (25 °C, 5 cm/min)	cm	≥100	≥ 100	D113-07
Softening Point (Ring & Ball)	°C	51	—	D36-06
Flash Point (Cleveland Open Cup)	°C	292	≥ 232	D92-12
Specific gravity at 25 °C	—	1.0375	—	D70-09
After Thin-Film Oven Test ASTM D 1754				
Retained Penetration of Residue (25°C, 100 gm, 5sec)	%	58	≥ 55	D5-06
Ductility at 25 °C, 5 cm/min, (cm)	cm	97	>25	D113-07

Table (2): Physical Properties of Aggregate.

Property	ASTM Specification No.	Results	SCRB Specification
Coarse aggregates			
Bulk Specific Gravity	C127-07	2.61	—
Apparent Specific Gravity	C127-07	2.601	—
Percent Water Absorption	C127-07	0.54	—
Percent Wear (Los Angeles Abrasion, %)	C535-09	15.79	30 Max
Fine aggregates			
Bulk Specific Gravity	C128-07	2.579	—
Apparent Specific Gravity	C128-07	2.632	—
Percent Water Absorption	C128-07a	0.952	—

Table (3): Physical Properties of Filler (Limestone Dust).

Property	Result
% Passing No.200	95
Specific gravity	2.71

Table (4): Physical and mechanical properties of SBS.

Property	SBS (styrene-butadiene styrene)
Physical state	solid
Density (Kg/m ³)	1247
Melting point, C°	197
Apparent	Light yellow

Table (5): Properties of glass fibers.

Property	Value
Density (gm/ cm ³)	2.5
Melting point (Co)	> 400
Poisson's Ratio	0.29
Tensile Strength (Gpa)	3.4
Modulus of Elasticity (Gpa)	72
Length (mm)	7
Diameter (mm)	0.21
Aspect Ratio	33.3



Figure 3. Glass fibers used in this research.

3.5 Aggregate Selection

The aggregate gradation was selected according to the [24] that subjected to the surface layer type 3A. Figure (4) show the selected aggregate gradation.

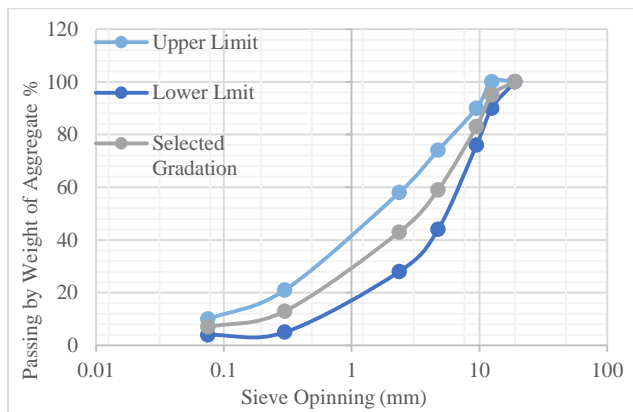


Figure 4. Aggregate gradation type.

4. Tests

4.1 Marshall test

The purpose of this test is to determine the optimum asphalt content (OAC), stability and air voids for asphalt concrete mixture. The preparation of cylindrical specimens with dimensions (101.6 mm) 4 inch in diameter and (63.5 mm) 2.5 inches in height. The Marshall Mould (consisting of a base plate and collar extension), and spatula, was heated on an oven to a temperature between (120-150 °C). The

asphalt mixture was placed in the preheated mould. Then, it was spaded vigorously with the heated spatula 15 times around the perimeter and ten times in the interior. The mixture's temperature immediately prior to compaction was between (142-146°C). Then, 75 blows on each face top and bottom of the specimen were applied with a compaction hammer of 4.535 kg sliding weight and a free fall of (457.2 mm) 18 inches. The specimen in the mould was left to cool at room temperature for 24 hours and then extracted from the mould by using a mechanical extractor. The bulk specific gravity and density were conducted according to [25]. The percent of air voids has been calculated from the formula shown below:

$$\% \text{Air Voids} = [1 - \text{Bulk sp.gr.} / \text{Max. Theo. sp.gr.}] * 100 \quad \dots\dots (1)$$

Marshall Stability and flow tests were performed on each specimen. The cylindrical specimen was immersed for 1/2 hour in 60 C° , after that the samples tested with (50.8. mm/min) loading rate, until the failure occurred. The peak load and flow rate was recorded to evaluate the sample behaviour. Figure (5) show the Marshall test machine and samples in the water path preparing to test.

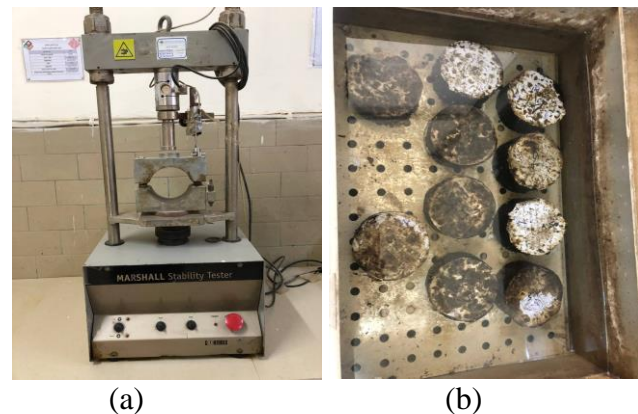


Figure 5. (a) Marshall test, (b) Marshall samples.

4.2 Semi-circular bending test (SCB)

The SCB test was used to assess the fracture characteristics. The specimen is configured with a 15 mm notch depth and shaped as a half-disc. The specimens were previously compressed to a thickness of 50 mm and a diameter of 150 mm. the specimen was cored with 6 inches (150) mm

from slabs of each type of mixtures, then Cut the core into two equal semi-circular specimens through the middle using the mechanical saw. Before the SCB test, the specimens were preconditioned at 15°C for 4 hours. The peak load attained and the specimens' deformation were observed. This test method evaluates the fracture energy (Gf) of the asphalt mixtures. The load is applied at a rate of 5 mm/min, and the load cell accuracy is (0.01 N). The LVDT is used to measure the vertical deformation. As shown in Figure 6.



Figure 6. SCB test.

4.3 Linear-Elastic Fracture Mechanics (LEFM)

In the phase framework of Linear Elastic Fracture Mechanics (LEFM), critical parameters such as the maximum stress (σ_{max}) and strain (ϵ_{max}) at failure, alongside key indicators like the specimen's geometric factor (GF), fracture toughness (KIC), and stiffness index (SI), were employed for analysis. These parameters offer valuable insights into the mechanical behavior of the material under stress.

The test evaluated the influence crack initiation and propagation. Following a sequence of mathematical computations, the simulation of crack development was carried out, focusing particularly on the determination of σ_{max} and ϵ_{max} at the point of failure.

Within LEFM, the stress intensity factor (K) serves as a fundamental measure to describe the stress field near the crack tip. When this factor

reaches the critical fracture toughness (KIC), failure is imminent. In semi-circular bending (SCB) tests, loading the specimen induces tensile stress at the notch tip, prompting crack initiation. The KIC value essentially represents the maximum stress intensity the material can endure before fracturing [26].

The values of σ_{max} and ϵ_{max} under failure conditions can be computed using Equations (1) and (2), as outlined in the European Standard [22] and supported by the findings of [27].

$$\bar{\sigma}_{max} = \frac{4.263 F_{max}}{D t} \quad \dots\dots (1)$$

$$\epsilon_{max} = \frac{\Delta w}{w} \times 100\% \quad \dots\dots (2)$$

Where the $\bar{\sigma}_{max}$ in N/mm², D and t are the diameter and thickness of the sample in mm, and ϵ_{max} is the maximum percentage of corresponding strain in %.

Linear Elastic Fracture Mechanics (LEFM) focuses on evaluating fracture behavior in scenarios where the plastic deformation zone is significantly smaller than the crack length. In this context, the stress intensity factor, commonly denoted as K, is used to characterize the fracture response of materials. The magnitude of this factor varies depending on the external loading conditions applied to the cracked specimen [28], [29].

A critical aspect of fracture mechanics is the material's resistance to crack propagation, expressed by its fracture toughness (K_{Ic}), which represents the threshold value of K beyond which failure occurs. Fracture toughness is a central parameter in LEFM research and is influenced by both the applied tensile stress and the specimen's geometric configuration, represented by the geometric factor (GF).

As loading progresses, the stress intensity factor increases, reaching a peak just before fracture initiation. The geometric factor (GF) can be calculated using Equation (3), while the corresponding fracture toughness (K_{Ic}) is derived from Equation (4), in accordance with [22] and the formulation presented by [30].

$$GF = -4.9965 + 155.58 \left(\frac{a}{w}\right) - 799.94 \left(\frac{a}{w}\right)^2 + 2141.9 \left(\frac{a}{w}\right)^3 - 2709.1 \left(\frac{a}{w}\right)^4 + 1398.6 \left(\frac{a}{w}\right)^5 \quad \dots\dots (3)$$

$$K_{Ic} = \bar{\sigma}_{max} * GF \quad \dots\dots (4)$$

Where KIc in $N/mm^{2/3}$, a and w is the notch depth and width of sample in mm.

The results of the fracture toughness (KIc) tests need to have a reasonable correlation with the results of the stiffness tests to ensure that the tensile strength obtained from the SCB test can be used to investigate the influence of asphalt-aggregate interaction on the mechanical behaviour of bituminous mixtures. This step is necessary to ensure that the tensile strength is adequate, [30].

The stiffness index (SI) measures displacement strength and indicates the difficulty of flexible deformation in asphalt materials. It represents the slope of the elastic stage of the load-displacement curve. It is determined by calculating the slope of the pre-peak slope upon reaching a maximal load of 50%. The Stiffness Index (SI) is a parameter used to quantify the material's ability to resist deformation under load. It is derived from the initial slope of the load-displacement curve, which represents the flexural stiffness of the specimen and can be calculated by using equation (5). [26], [31], [32].

$$SI = \frac{dF}{d\Delta W} \quad \dots\dots (5)$$

Where dF is the increment in load in kN and $d\Delta W$ is increment in displacement in mm.

4.4 Fracture Toughness Modulation Index (FTMI)

The Fracture Toughness Modulation Index (FTMI) is a newly proposed fracture parameter designed to assess the post-peak energy dissipation ability of asphalt mixtures in relation to their initial stiffness. It specifically quantifies the modulation of fracture toughness due to polymer modification, reflecting the balance between energy absorption and stiffness degradation after crack initiation. This parameter is sensitive to the ductile behavior imparted by modifiers.

The (FTMI) aims to represent how effectively a material sustains post-peak loading after crack initiation, relative to its initial stiffness. In other words, it reflects the ductility after cracking while penalizing materials that are too stiff and brittle.

In fracture mechanics, the post-peak softening area indicates energy dissipation due to microcrack growth, plasticity, and viscoelastic flow. In modified asphalt, this area increases due to the toughening effect of polymers.

Hence, FTMI is constructed to compare:

- The residual energy after peak load (positive behavior),
- To the initial elastic stiffness and deformation range in softening (controlling for material rigidity).

To calculate this index parameter, we need to normalized measure of energy dissipation, as shown in equation (6).

$$FTMI = \frac{\text{Energy absorbed after cracking}}{\text{Material rigidity and softening length}} * 100\% \quad \dots\dots (6)$$

The term of (Energy absorbed after cracking) can be define as Residual Work (Post-Peak Fracture Energy). This represents the area under the curve from the peak to failure, capturing the fracture propagation and energy dissipation after crack initiation. This concept can be represented mathematically in equation (7):

$$W_r = \int_{\Delta W_c}^{\Delta W_f} F(\Delta W) d\Delta W \quad \dots\dots (7)$$

The term of material rigidity and softening length can define as it's the combined effect of Stiffness Index (SI) during Deformation Range in Softening Phase (LEFM) and can be represented in equation (8).

$$\text{Material rigidity and softening length} = SI \times \Delta W_s \times a \quad \dots\dots (8)$$

Where $F(\Delta W)$ be the load as a function of vertical deformation ΔW , ΔW_c is the critical displacement at peak load F_{max} , ΔW_f is the final deformation where fracture is essentially complete, a the notch depth, and ΔW_s represent the deformation in the elastic range (LEFM) which can be represented in equation (9).

$$\Delta W_s = \Delta W_f - \Delta W_c \quad \dots\dots (9)$$

The final term which can be used to calculate the index which is Dimensionless (or normalized index) shown in equation (10), the high FTMI represent to High energy dissipation after cracking; good ductility; polymer modification effective, and low FTMI represent to Sharp brittle failure; stiff but not tough.

$$FTMI = \frac{Wr}{SI * \Delta Ws * a} * 100\% \quad \dots\dots (10)$$

4.4 Energy-Based Brittleness Index (EBI)

The Energy-Based Brittleness Index (EBI) is intended to evaluate the ratio of load-carrying capacity to fracture energy. A material that reaches a high peak load but fails abruptly absorbs less energy before failure, indicating brittle behavior. [33] showed that Brittleness Index (BI) for peak point in equation (11).

$$BI = (\sigma_a^2 - \sigma_b^2) / 2E \quad \dots\dots (11)$$

Based on [34] can obtained the equations. Equation (12) obtained By Express Wf in Terms of σ (Griffith's Approach).

$$Wf \propto \frac{\sigma f^2}{E} \cdot Ac \quad \dots\dots(12)$$

For a given specimen geometry, Ac and E are constants, so $Wf \propto \sigma^2 \propto F_{max}^2$.

The Elastic energy at failure (Ue) can be define as shown in equation (13):

$$Ue = \frac{1}{2} F_{max} \cdot \delta_{max}$$

For For linear elasticity, $\delta_{max} \propto F_{max}$, so that

$$Ue \propto \frac{1}{2} F_{max}^2 \quad \dots\dots (13)$$

The final equation to define (EBI) which can be calculate by using the equation of (14).

$$EBI = \frac{\text{Elastic energy potential}}{\text{Fracture energy}} = \frac{F_{max} * F_{max}}{2Wf} \quad \dots (14)$$

Where F_{max}^2 in [kN²] reflects peak load squared (brittle behavior), and $2Wf$ [kN·mm] normalizes by total energy absorbed (reflects how much energy is absorbed before fracture). Thus, EBI acts like a normalized stiffness to energy ratio the higher the index, the more brittle the response, and have the same stiffness unit (KN/mm).

The High EBI value refer to High stress, low energy and that mean brittle behavior. On the other hand, the Low EBI refer to Moderate stress, high energy and that mean ductile, desirable in modified asphalt.

5. Results

5.1 Marshall test

A collection of Marshall tests (stability, density and Air voids) was analyzed to find the OAC for four asphalt concrete mixtures [(AC 40- 50), modified AC (40-50) with 2, 4 and 6 %

SBS] as shown in table 6. Five different asphalt contents for each mixture range from 4 to 6 percent (by weight of total mix) with an increment of 0.5 %. Three specimens were prepared and tested for each mixture using aggregate (12.5 mm nominal maximum size gradation). The average of the following values was taken to adopt the OAC for wearing the course layer.

After finding OAC for conventional and modified asphalt, glass fibers added by (0.25,0.5,0.75,1) % of total mixture for conventional and modified asphalt. The OAC found according to:

Max bulk density, Max stability, 4% Air voids, Flow \rightarrow (2-4) mm. Further, Marshall Properties (VMA and VFA) were measured to check Whether to meet Iraqi specifications of [24].

The OAC was (4.91) % for virgin AC (40-50), (4.86) % for modified AC (40-50) with 2% SBS, (4.833) % for modified AC (40-50) with 4% SBS and (4.78) % for modified AC (40-50) with 6% SBS. The modified AC (40-50) with 6% SBS does not meet the requirements of [24] in flow value. Marshall properties for OAC except 6% modified with SBS, meet the Iraqi requirement specification of [24]. As a result, modified asphalt with 4% SBS additive was choose as optimum additive which produce best mechanical properties in range of the Iraqi requirement specification as shown in table (4.1).

The results show that adding SBS to conventional asphalt leads to reduce the OAC and increasing stability by 9.73%, 23% and 35.4% for modified asphalt with 2%,4% and 6% respectively compared with conventional asphalt. On other hand; adding SBS to conventional asphalt leads to increasing in air voids in total mixture (AV%), were air voids increased by 10.81%,14.86% and 24.32% for modified asphalt with 2%,4% and 6% respectively compared with conventional asphalt. All other results were listed in table After finding the OAC for conventional asphalt and ideal additive of modified asphalt with SBS (4%) by weight of asphalt. Glass fibers added to the two types of asphalt with (0.25, 0.5, 0.75 and

1%) by weight of mixture to calculate the properties, Such behavior of materials complies with the findings of [35], [36] optimum glass fiber content for each type. Three samples were tested to each percent additive and average result recorded.

The results show that increasing trend in stability with 0.25% and 0.5 % by weight of total mixture for both conventional and modified asphalt, then the result shows reduction in stability values with 0.75% and 1% by weight of total mixture for both conventional and modified asphalt. All the results listed in tables 7 and 8 for

conventional and modified asphalt respectively. Such behavior of materials complies with the findings of [37], [38].

5.2 Semi-circular bending test

After applying load test. The data logger with two displacement sensors and load cell provide data and exports 4 columns of data (Load cell, LVDT 1, LVDT 2, Time). The exported data drawn with (X, Y) coordinates. As shown in figure 7 which represent the load-displacement curve.

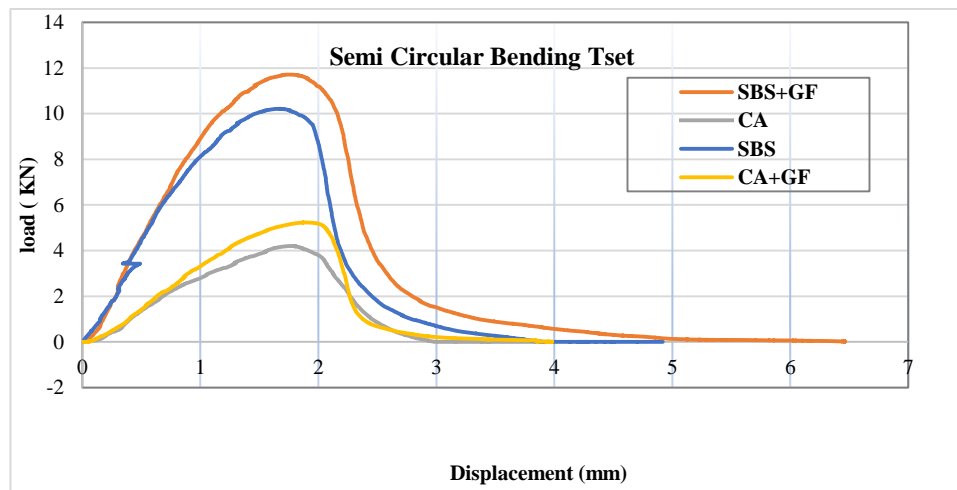


Figure 7. Load-displacement curve for SCB test.

Table (6): Marshall Properties of OAC for conventional and Modified AC (40-50).

Marshall Properties	Mix Type				(SCR, 2003) Specifications
	conventional AC (40-50)	Modified With 2%SBS	Modified With 4%SBS	Modified with 6%SBS	
Stability (kN)	11.3	12.4	13.9	15.3	8 min.
Bulk Density (gm/cm ³)	2.322	2.319	2.317	2.309	-
Flow (mm)	3.4	2.9	2.4	1.95	2-4
AV (%)	3.7	4.1	4.25	4.6	3-5
VMA (%)	16.2	16.27	16.32	16.6	14 min.
VFA (%)	77.16	74.8	73.95	72.28	70-85
OAC (%)	4.91	4.86	4.833	4.78	4-6

5.2.1 Linear-Elastic Fracture Mechanics (LEFM)

The Linear Elastic Fracture Mechanics (LEFM) results show a clear enhancement in

fracture resistance and stiffness with the incorporation of glass fibers (GF) and styrene-butadiene-styrene (SBS) polymer into asphalt mixtures. The maximum load and maximum displacement

Table (7): Marshall Properties of glass fibers for conventional AC (40-50).

Marshall Properties	Mix Type					(SCR, 2003) Specifications
	conventional AC (40-50)	0.25% GF	0.5% GF	0.75% GF	1% GF	
Stability (kN)	11.3	12.6	13.8	13.5	13	8 min.
Bulk Density (gm/cm ³)	2.322	3.18	2.9	3.12	3.45	-
Flow (mm)	3.4	2.332	2.348	2.341	2.321	2-4
AV (%)	3.7	3.67	3.63	3.72	3.84	3-5
VMA (%)	16.2	15.038	14.455	14.710	15.439	14 min.
VFA (%)	77.16	75.595	74.88	74.7118	75.128	70-85

Table (8): Marshall Properties of glass fibers for Modified AC with SBS.

Marshall Properties	Mix Type					(SCR, 2003) Specifications
	Modified AC (40-50)	0.25% GF	0.5% GF	0.75% GF	1% GF	
Stability (kN)	13.9	14.3	15.6	15.1	14.1	8 min.
Bulk Density (gm/cm ³)	2.4	2.34	2.3	2.36	3.11	-
Flow (mm)	2.31	2.321	2.328	2.319	2.302	2-4
AV (%)	4.25	3.91	3.46	3.88	4.12	3-5
VMA (%)	15.771	15.370	15.115	15.443	16.063	14 min.
VFA (%)	73.053	74.561	77.109	74.876	74.351	70-85

increased progressively from conventional asphalt (CA) to CA+GF, SBS, and SBS+GF, indicating improved load-bearing capacity and deformation tolerance. The fracture toughness (K_{Ic}) increased by approximately 30% when GF was added to CA (from 10.16 to 13.22 N·mm), primarily due to the crack bridging mechanism of glass fibers, which delays crack propagation and dissipates more fracture energy. This agrees with previous studies reporting that glass fibers enhance asphalt mixture tensile strength and fracture work density through fiber–matrix interlock and load transfer across cracks. The use of SBS polymer resulted in a more significant improvement in fracture toughness by 125% (25.81 N·mm), reflecting its ability to increase mixture elasticity, reduce brittleness, and absorb higher strain energy before fracture. SBS modification has been widely reported to improve low-temperature cracking resistance

and fatigue life by forming an elastic network within the bitumen matrix [16], [39], [40].

The combination of SBS and GF yielded the highest fracture toughness (29.60 N·mm) and stiffness index (6.00 kN/mm) which increased by 191% and 142% respectively compared with CA, indicating a synergistic effect: SBS enhances ductility and flexibility, while GF provides structural reinforcement, resulting in a balanced mixture with high strength and high energy absorption capacity. Such synergy between polymer modification and fiber reinforcement is consistent with findings in composite material toughening mechanisms [41], [42].

The results confirm that hybrid reinforcement using both SBS and GF can

significantly improve fracture resistance and stiffness compared to single-modified or unmodified mixtures, in that the fracture energy increased with increasing the glass fiber content and fracture angle. The reason for the increase in fracture energy, as already mentioned, is due to the increase of the interlock between the aggregates, fibers, and bitumen. Therefore, the

higher the amount of fiber, the higher the resistance to the forces and stress. Typically, the toughness of the specimens will increase, which will increase the surface area below the curve and, as a result, increase the fracture energy [40], [43].

Table (9): (LEFM) parameters with Stiffness Index.

Asphalt mixture type	SCB parameters (LEFM)				Geometric factor (GF)	fracture toughness (K_{Ic}) ($N/mm^{2/3}$)	Stiffness Index (SI) (KN/mm)
	Maximum load (KN)	Maximum displacement (Δw)	$\bar{\sigma}$ max (N/mm^2)	ϵ max			
CA	4.1999	1.7	2.387	1.13	4.44707	10.1615	2.47052
CA+GF	5.2316	1.8	2.973	1.20	4.44707	13.2210	2.90644
SBS	10.2124	1.9	5.804	1.26	4.44707	25.8107	5.37494
SBS+GF	11.7124	1.95	6.657	1.32	4.44707	29.6041	6.00635

5.2.2 Fracture Toughness Modulation Index (FTMI) and Energy-Based Brittleness Index (EBI)

The calculated Fracture Toughness Modulation Index (FTMI) values provide quantitative insight into the post-peak fracture behavior of the different asphalt mixtures evaluated through the SCB test. FTMI reflects the material's capacity to dissipate energy after crack initiation, normalized by stiffness and softening deformation length.

The FTMI results Table 10 reveal distinct fracture behavior trends among the tested asphalt mixtures. Conventional Asphalt (CA) achieved the highest FTMI value (45.77 mm), which reflects its lower stiffness. However, this high FTMI does not indicate superior fracture resistance; rather, it results from the low stiffness denominator in the FTMI formulation, despite modest residual fracture work.

The addition of glass fibers to conventional asphalt (CA+GF) significantly reduced FTMI (24.79 mm). Although fiber reinforcement improved stiffness and peak load, it also shortened the post-peak softening zone, yielding a more brittle fracture response.

SBS modification resulted in an FTMI of 34.80 mm, representing a balanced combination of stiffness, fracture energy, and post-peak ductility. The SBS+GF mixture displayed the highest peak load and stiffness but recorded a slightly lower FTMI (31.62 mm) than SBS alone, indicating a shift toward a stiffer, less ductile fracture mode.

Overall, FTMI captured the trade-off between stiffness and ductility, highlighting SBS as the optimal single modifier for balanced fracture performance, while SBS+GF prioritized stiffness and strength at the expense of ductility.

Table (10): Fracture Toughness Modulation Index (FTMI) parameters.

Asphalt mixture type	(FTMI) parameters					Material rigidity & softening length. (mm)	FTMI
	Maximum load (KN)	Maximum displacement (Δw_c)	(Δw_f) (mm)	(Δw_s) (mm)	Wr (N.mm)		
CA	4.1999	1.7	3	1.3	2205.2	4817.514	45.77464
CA+GF	5.2316	1.8	3.85	2.05	2215.4	8937.303	24.78823
SBS	10.2124	1.9	3.9	2.2	6172.6	17737.30	34.80010
SBS+GF	11.7124	1.95	5.2	3.25	9259.4	29280.95	31.62260

The Energy-Based Brittleness Index (EBI) quantifies the relationship between a mixture's peak load capacity and its ability to absorb fracture energy before failure. Higher EBI values indicate mixtures that exhibit relatively higher strength but lower relative ductility, implying a shift toward brittle fracture behavior.

The Conventional Asphalt (CA) mixture recorded the lowest EBI value (1.398), reflecting its low peak load capacity and moderate total fracture energy. This low index is consistent with CA's flexible but structurally weaker nature; it fails at lower loads but exhibits a longer post-peak softening phase.

The addition of glass fibers to conventional asphalt (CA+GF) increased EBI to 1.770, indicating a reduction in relative ductility. The improvement in peak load (from 4.20 kN to 5.23 kN) was accompanied by a slight increase in total fracture work, but the proportional gain in

strength outweighs the energy gain, shifting the fracture mode toward greater brittleness.

The SBS-modified mixture exhibited a substantial increase in EBI (3.126), driven by significant gains in both peak load and fracture energy. While SBS modification improves fracture resistance, the higher EBI suggests that the enhancement in load-carrying capacity is proportionally greater than the improvement in energy absorption, producing a stiffer and relatively more brittle profile compared to CA.

The SBS+GF mixture achieved the highest peak load (11.71 kN) and the highest fracture energy (21.71 kN·mm), yielding the highest EBI (3.160). However, the difference in EBI between SBS+GF and SBS alone is marginal. This suggests that while the combined reinforcement improves absolute mechanical performance, it does not drastically alter the balance between strength and fracture energy, meaning brittleness is similar to SBS alone.

Table (11): EBI calculations.

Asphalt mixture type	(EBI) parameters		(EBI)
	Maximum load (KN)	Wf (KN/mm)	
CA	4.1999	6.31	1.39771
CA+GF	5.2316	7.73	1.77035
SBS	10.2124	16.68	3.12629
SBS+GF	11.7124	21.71	3.15938

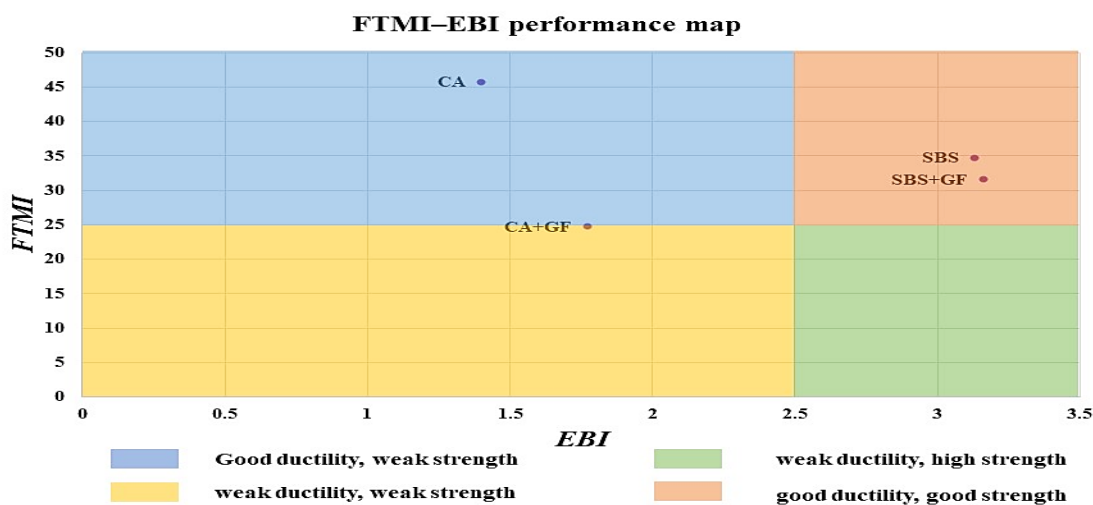


Figure 7. Matrix evaluation based on FTMI and EBI.

FTMI and EBI reveal the trade-off between ductility and brittleness in asphalt mixtures:

- CA: High FTMI, low EBI → flexible but structurally weak; prone to large deformations under load.
- CA+GF: Low FTMI, moderate EBI → stronger but less ductile; increased brittleness risk.
- SBS: Balanced FTMI and high EBI → strong with reasonable ductility; good all-round fracture resistance.
- SBS+GF: Slightly reduced FTMI, highest EBI → maximum strength but reduced ductility; risk of brittle failure if not designed for reflective crack control.

6. Conclusions

Overall, the experimental program confirmed that both polymer modification and fiber reinforcement can enhance the mechanical performance of asphalt concrete, but the improvement mechanism depends on the modifier type and dosage.

- Marshall mix design indicated that increasing styrene–butadiene–styrene content lowered the optimum asphalt content and increased stability.
- Nevertheless, the highest polymer dosage did not satisfy the specification flow range, which highlights that excessive polymer stiffening can compromise constructability and performance compliance.
- Glass fibers improved Marshall stability up to an intermediate content and then reduced stability at higher additions, suggesting that fiber clustering or reduced workability may offset reinforcement benefits when the fiber content becomes excessive.
- Semi-circular bending results, interpreted using linear elastic fracture mechanics, showed a clear progression in cracking resistance from the conventional mixture to the modified mixtures. Fracture

toughness increased from about 10.16 N/mm^{2/3} for the conventional mixture to 13.22 N/mm^{2/3} with glass fibers, and to 25.81 N/mm^{2/3} with polymer modification. The combined polymer–fiber mixture produced the highest fracture toughness (29.60 N/mm^{2/3}) and stiffness index (6.01 kN/mm), indicating a synergistic effect in which the polymer improved ductility and strain tolerance while fibers provided crack-bridging and load transfer.

- The fracture toughness modulation index and the energy-based brittleness index were useful complementary indicators for post-peak behavior. Although the conventional mixture exhibited the highest modulation index due to its low stiffness, it also showed the lowest brittleness index, reflecting a weak but more deformable response. Fiber addition to the conventional mixture reduced the modulation index and increased brittleness, whereas polymer modification provided a more favorable balance. The combined polymer–fiber mixture achieved the highest strength and stiffness, with only a slight reduction in post-peak ductility compared with polymer-only modification.

Based on these findings, polymer modification is recommended when balanced fracture resistance is required, while hybrid polymer–fiber reinforcement is appropriate when maximizing stiffness and load capacity is the design priority. Further validation over a wider temperature range and under cyclic fatigue and moisture conditioning is recommended to support field implementation.

References

- [1] D. Llopis-Castelló et al., “Influence of Pavement Structure, Traffic, and Weather on Urban Flexible Pavement Deterioration,” *Sustainability*, vol. 12, no. 22, Nov. 2020, doi: 10.3390/su12229717.
- [2] J. Li et al., “Research progresses of fibers in asphalt and cement materials: A review,” *Journal of Road*

- Engineering, vol. 3, no. 1, pp. 35–70, Mar. 2023, doi: 10.1016/j.jreng.2022.09.002.
- [3] C. Riccardi, I. Indacochea, D. Wang, P. Lastra-González, A. Cannone Falchetto, and D. Castro-Fresno, “Low temperature performances of fiber-reinforced asphalt mixtures for surface, binder, and base layers,” *Cold Regions Science and Technology*, vol. 206, p. 103738, Feb. 2023, doi: 10.1016/j.coldregions.2022.103738.
- [4] Y. Hui et al., “Recent Advances in Basalt Fiber Reinforced Asphalt Mixture for Pavement Applications,” *Materials*, vol. 15, no. 19, Oct. 2022, doi: 10.3390/ma15196826.
- [5] N. Mashaan et al., “Bituminous Pavement Reinforcement with Fiber: A Review,” *CivilEng*, vol. 2, no. 3, pp. 599–611, Jul. 2021, doi: 10.3390/civileng2030033.
- [6] S. Tayfur, H. Ozen, and A. Aksoy, “Investigation of rutting performance of asphalt mixtures containing polymer modifiers,” *Construction and Building Materials*, vol. 21, no. 2, pp. 328–337, Feb. 2007, doi: 10.1016/j.conbuildmat.2005.08.014.
- [7] S. Anjan kumar and A. Veeraragavan, “Dynamic mechanical characterization of asphalt concrete mixes with modified asphalt binders,” *Materials Science and Engineering: A*, vol. 528, no. 21, pp. 6445–6454, Aug. 2011, doi: 10.1016/j.msea.2011.05.008.
- [8] J. Q. Chen, A. J. Li, M. Q. Jin, M. N. Zheng, and W. Y. Yang, “Study on Low Temperature Performance of SBS Modified Asphalt and its Mixture,” *Applied Mechanics and Materials*, vol. 587–589, pp. 1332–1336, 2014, doi: 10.4028/www.scientific.net/AMM.587-589.1332.
- [9] P. Lin, W. Huang, Y. Li, N. Tang, and F. Xiao, “Investigation of influence factors on low temperature properties of SBS modified asphalt,” *Construction and Building Materials*, vol. 154, pp. 609–622, Nov. 2017, doi: 10.1016/j.conbuildmat.2017.06.118.
- [10] E. Iskender, A. Aksoy, and H. Ozen, “Indirect performance comparison for styrene–butadiene–styrene polymer and fatty amine anti-strip modified asphalt mixtures,” *Construction and Building Materials*, vol. 30, pp. 117–124, May 2012, doi: 10.1016/j.conbuildmat.2011.11.027.
- [11] T. W. Kim, J. Baek, H. J. Lee, and J. Y. Choi, “Fatigue performance evaluation of SBS modified mastic asphalt mixtures,” *Construction and Building Materials*, vol. 48, pp. 908–916, Nov. 2013, doi: 10.1016/j.conbuildmat.2013.07.100.
- [12] A. Modarres, “Investigating the toughness and fatigue behavior of conventional and SBS modified asphalt mixes,” *Construction and Building Materials*, vol. 47, pp. 218–222, Oct. 2013, doi: 10.1016/j.conbuildmat.2013.05.044.
- [13] A. R. Copeland, J. Youtcheff, and A. Shenoy, “Moisture Sensitivity of Modified Asphalt Binders: Factors Influencing Bond Strength,” *Transportation Research Record*, vol. 1998, no. 1, pp. 18–28, Jan. 2007, doi: 10.3141/1998-03.
- [14] Y. Gong, J. Xu, R. Chang, and E. Yan, “Effect of water diffusion and thermal coupling condition on SBS modified asphalts’ surface micro properties,” *Construction and Building Materials*, vol. 273, p. 121758, Mar. 2021, doi: 10.1016/j.conbuildmat.2020.121758.
- [15] S. M. Abtahi, M. Sheikhzadeh, and S. M. Hejazi, “Fiber-reinforced asphalt-concrete – A review,” *Construction and Building Materials*, vol. 24, no. 6, Art. no. 6, Jun. 2010, doi: 10.1016/j.conbuildmat.2009.11.009.
- [16] H. Ziari, M. R. M. Aliha, A. Moniri, and Y. Saghafi, “Crack resistance of hot mix asphalt containing different percentages of reclaimed asphalt pavement and glass fiber,” *Construction and Building Materials*, vol. 230, p. 117015, Jan. 2020, doi: 10.1016/j.conbuildmat.2019.117015.
- [17] S. Pirmohammad, M. Abdi, and M. R. Ayatollahi, “Effect of support type on the fracture toughness and energy of asphalt concrete at different temperature conditions,” *Engineering Fracture Mechanics*, vol. 254, p. 107921, Sep. 2021, doi: 10.1016/j.engfracmech.2021.107921.
- [18] S. Pirmohammad, Y. Majd Shokorlou, and B. Amani, “Fracture Resistance of HMA Mixtures Modified with Nanoclay and Nano- Al_2O_3 ,” *J. Test. Eval.*, vol. 47, no. 5, pp. 3289–3308, Sep. 2019, doi: 10.1520/JTE20180919.
- [19] M. Ameri, S. V. Abdipour, A. R. Yengejeh, M. Shahsavari, and A. A. Yousefi, “Evaluation of rubberised asphalt mixture including natural Zeolite as a warm mix asphalt (WMA) additive,” *International Journal of Pavement Engineering*, vol. 24, no. 2, p. 2057977, Jan. 2023, doi: 10.1080/10298436.2022.2057977.
- [20] A. Yousefi, S. Pirmohammad, and S. Sobhi, “Fracture Toughness of Warm Mix Asphalts Containing Reclaimed Asphalt Pavement,” *Journal of Stress Analysis*, vol. 5, no. 1, pp. 85–98, Sep. 2020, doi: 10.22084/jrstan.2020.22325.1153.

- [21] A. A. Yousefi, S. Sobhi, M. R. M. Aliha, S. Pirmohammad, and H. F. Haghshenas, "Cracking Properties of Warm Mix Asphalts Containing Reclaimed Asphalt Pavement and Recycling Agents under Different Loading Modes," *Construction and Building Materials*, vol. 300, p. 124130, Sep. 2021, doi: 10.1016/j.conbuildmat.2021.124130.
- [22] B. EN, "12697-44. Bituminous Mixtures-Test Methods for Hot Mix Asphalt-part 44: Crack propagation by semi-circular bending test," British Standard London, United Kingdom, 2010.
- [23] ASTM D8044-16, "Standard Method of Test for Evaluation of Asphalt Mixture Fracture Resistance Using the Semi-Circular Bend (SCB) Test at Intermediate Temperature." Astm., 2016. [Online]. Available: 1-7
- [24] R. E. SCRB, "Standard Specifications for Roads and Bridges, Section R/9, Hot-Mix Asphaltic Concrete Pavement," The State Corporation for Roads and Bridges, Ministry of Housing and Construction, 2003.
- [25] ASTM D6927, "Standard Test Method for Marshall Stability and Flow of Asphalt Mixtures." Accessed: Jul. 01, 2025. [Online]. Available: <https://store.astm.org/d6927-15.html>
- [26] E. Zegeye, Le ,Jia-Liang, Turos ,Mugur, and M. and Marasteanu, "Investigation of size effect in asphalt mixture fracture testing at low temperature," *Road Materials and Pavement Design*, vol. 13, no. sup1, pp. 88–101, Jun. 2012, doi: 10.1080/14680629.2012.657064.
- [27] J. Wei et al., "Experimental Research on the Effect of Fiberglass on the Performance of Epoxy Asphalt Concrete," *Sustainability*, vol. 14, no. 22, p. 14724, Jan. 2022, doi: 10.3390/su142214724.
- [28] X. Chen, "Use of Semi-Circular Bend Test to Characterize Fracture Properties of Asphalt Concrete with Virgin and Recycled Materials - ProQuest," The Pennsylvania State University ProQuest Dissertations & Theses. Accessed: Dec. 21, 2025. [Online]. Available: <https://www.proquest.com/openview/8c9c0b90775c326b30f0aae79bc9ded8/1?pq-origsite=gscholar&cbl=18750&diss=y>
- [29] G. Nsengiyumva, "Development of Semi-circular Bending (SCB) Fracture Test for Bituminous Mixtures," Department of Civil and Environmental Engineering: Dissertations, Theses, and Student Research, Dec. 2015, [Online]. Available: <https://digitalcommons.unl.edu/civilengdiss/87>
- [30] Y. Chen, S. Xu, G. Tebaldi, and E. Romeo, "Role of mineral filler in asphalt mixture," *Road Materials and Pavement Design*, vol. 23, no. 2, pp. 247–286, Feb. 2022, doi: 10.1080/14680629.2020.1826351.
- [31] R. Bonaquist, B. Paye, and C. Johnson, "Application of intermediate temperature semi-circular bending test results to design mixtures with improved load-associated cracking resistance," *Road Materials and Pavement Design*, vol. 18, no. sup4, pp. 2–29, Nov. 2017, doi: 10.1080/14680629.2017.1389069.
- [32] Y. Meng et al., "A review on evaluation of crack resistance of asphalt mixture by semi-circular bending test," *Journal of Road Engineering*, vol. 3, no. 1, pp. 87–97, Mar. 2023, doi: 10.1016/j.jreng.2022.07.003.
- [33] D. Zhang, P. G. Ranjith, and M. S. A. Perera, "The brittleness indices used in rock mechanics and their application in shale hydraulic fracturing: A review," *Journal of Petroleum Science and Engineering*, vol. 143, pp. 158–170, Jul. 2016, doi: 10.1016/j.petrol.2016.02.011.
- [34] T. L. Anderson and T. L. Anderson, *Fracture Mechanics: Fundamentals and Applications*, Third Edition, 3rd ed. Boca Raton: CRC Press, 2005. doi: 10.1201/9781420058215.
- [35] Al-Jumaili, "ISSN 2320-5407 International Journal of Advanced Research (2015), Volume 3, Issue 11, 1224 – 1232," *International Journal of Advanced Research*, vol. 3, no. 11, 2015.
- [36] S. A. Jasim and M. Q. Ismael, "Marshall Performance and Volumetric Properties of Styrene-Butadiene-Styrene Modified Asphalt Mixtures," *Civ Eng J*, vol. 7, no. 6, Art. no. 6, Jun. 2021, doi: 10.28991/cej-2021-03091709.
- [37] M. S. Eisa, M. E. Basiouny, and M. I. Dalooob, "Effect of adding glass fiber on the properties of asphalt mix," *Int. J. Pavement Res. Technol.*, vol. 14, no. 4, Art. no. 4, Jul. 2021, doi: 10.1007/s42947-020-0072-6.
- [38] T. T. Khaled, A. I. Kareem, S. A. Mohamad, R. Kh. S. Al-Hamd, and A. Minto, "The Performance of Modified Asphalt Mixtures with Different Lengths of Glass Fiber," *Int. J. Pavement Res. Technol.*, May 2024, doi: 10.1007/s42947-024-00443-x.
- [39] E. Yalcin et al., "Evaluation of asphalt anti-cracking performance of SBS polymer with SCB method and deep learning," *Heliyon*, vol. 10, no. 20, Oct. 2024, doi: 10.1016/j.heliyon.2024.e39613.
- [40] J. Wei, J. Mao, Y. Han, P. Li, W. Wu, and C. Yi, "Influence of Different Fibers on Performance of Bitumen Binders and Thin-Overlay Bitumen Mixtures," *Applied Sciences*, vol. 15, no. 1, Art. no. 1, Jan. 2025, doi: 10.3390/app15010022.

- [41]S. H. Khanghahi and A. Tortum, “Determination of the Optimum Conditions for Gilsonite and Glass Fiber in HMA under Mixed Mode I/III Loading in Fracture Tests,” *J. Mater. Civ. Eng.*, vol. 30, no. 7, p. 04018130, Jul. 2018, doi: 10.1061/(ASCE)MT.1943-5533.0002278.
- [42]F. Morea and R. Zerbino, “Improvement of asphalt mixture performance with glass macro-fibers,” *Construction and Building Materials*, vol. 164, pp. 113–120, Mar. 2018, doi: 10.1016/j.conbuildmat.2017.12.198.
- [43]H. Akram, H. A. Hozayen, and F. Khodary, “Experimental Study of the Effect of High Length of Glass and Polypropylene Fibers on Asphalt Mixture Characteristics,” *Sohag Engineering Journal*, Apr. 2025, doi: 10.21608/sej.2025.358585.1074.